

NATIONAL AIR INTELLIGENCE CENTER



THE STUDY OF FATIGUE BEHAVIOR FOR IMPACTED ARALL COUNTERMEASURES

by

Guo Yajun, Shao Yujun, Zheng Ruigi



Approved for public release:
distribution unlimited

19960104 050

HUMAN TRANSLATION

NAIC-ID(RS)T-0377-95 21 November 1995

MICROFICHE NR: 95c000714

THE STUDY OF FATIGUE BEHAVIOR FOR IMPACTED ARALL
COUNTERMEASURES

By: Guo Yajun, Shao Yujun, Zheng Ruigi

English pages: 6

Source: Hangkong Xuebao, Vol. 15, Nr. 12, December 1994;
pp. 1532-1535.

Country of origin: China

Translated by: SCITRAN

F33657-84-D-0165

Requester: NAIC/TATV/Beverly G. Brown

Approved for public release: distribution unlimited.

Accession For	
NTIS CRA&I	<input checked="" type="checkbox"/>
DTIC TAB	<input type="checkbox"/>
Unannounced	<input type="checkbox"/>
Justification	
By	
Distribution /	
Availability Codes	
Dist	Avail and/or Special
A-1	

THIS TRANSLATION IS A RENDITION OF THE ORIGINAL FOREIGN TEXT WITHOUT ANY ANALYTICAL OR EDITORIAL COMMENT STATEMENTS OR THEORIES ADVOCATED OR IMPLIED ARE THOSE OF THE SOURCE AND DO NOT NECESSARILY REFLECT THE POSITION OR OPINION OF THE NATIONAL AIR INTELLIGENCE CENTER.

PREPARED BY:

TRANSLATION SERVICES
NATIONAL AIR INTELLIGENCE CENTER
WPAFB, OHIO

ABSTRACT As far as impact damage mechanisms with regard to free ARALL and two types of prestressed ARALL laminates are concerned, surface observations and test measurement analysis without damage were carried out with respect to the propagation of impact damage during fatigue processes. Cumulative fatigue damage models were set up for laminates after impact. Probes were done with regard to the influences of prestressing on fatigue properties after ARALL laminate impact.

KEY WORDS Laminates Impact resistance Fatigue tests

Chinese Library Classification No. V250.3

GRAPHICS DISCLAIMER

All figures, graphics, tables, equations, etc. merged into this translation were extracted from the best quality copy available.

ARALL laminates are glued aromatic fiber/aluminum alloy laminates. They have already achieved applications in such parts as aircraft wing skins, cargo compartment doors, as well as forward fuselage sections, and so on. Weight reductions respectively reached 33%, 23%, and 25%. Fatigue life was clearly increased. However, the main cause blocking widespread applications of ARALL laminates is sensitivity to impact and puncture. Free ARALL laminate residual stresses are large. This severely influences the dynamic properties of ARALL laminates-- particularly, fatigue properties. Therefore, research on fatigue properties of ARALL laminates after impact was launched, and explorations of the influences of prestressing on laminate dynamic properties is very significant.

1 System Tests

1.1 Samples

Taking 3/2 structure ARALL laminate, it was worked into an impact sample 250mm long and 80mm wide. The sample nominal thickness was approximately 1.4mm. One type of sample was chosen without prestressing (ps0). Two types of samples had prestressing (ps1: 450MPa and ps2: 790MPa).

1.2 Laminate impact tests were carried out on a controlled hammer drop type test apparatus [1]. The impact samples were placed on the support clamping apparatus. The square aperture dimensions of the support clamping apparatus were 75mmx75mm. Between the samples and the clamp plates, a rubber sleeve ring liner was placed. Bolts were used to tighten it down. The impact body vertically struck the center of the sample using a free falling body method. The mass of the impact body was 2.5kg. The drop height was 0.4m. The impact energy amounted to 9.81J. /1533

1.3 Test Measurement Experiments Without Damage

In all cases, internal laminate damage was detected with the use of X ray penetration. Sample surface cracking was recorded with the use of a camera.

1.4 Fatigue Tests

Samples after impact go through fatigue tests directly on an MTS810 materials testing apparatus after passing through test measurements without losses. Sine wave loads are added. Fatigue test parameters are: $\sigma_{max} = 160$ MPa, $f=15$ Hz, $R=0.1$. During testing processes, monitors point out maximum and minimum values for sample loads and displacements under numbers of cycle iterations. Use is made of the equation below to calculate laminate dynamic stiffness.

$$K_d = (P_{max} - P_{min}) / (\delta_{max} - \delta_{min}) \quad (1)$$

In this, P_{max} , P_{min} and δ_{max} , δ_{min} are respectively maximum and minimum values for load and displacement. K_d is laminate dynamic stiffness.

2 Test Results and Their Analysis

2.1 ARALL Laminate Impact Damage Mechanisms

Fig.1 and Fig.2 are, respectively, outside photographic views and X ray penetration photographs of three types of samples after impact. It can be seen that ARALL laminate impact damage primarily appears as aromatic fiber breaks in the vicinity of impact points. There is aluminum layer plastic deformation as well as delamination between aluminum layers and aromatic fiber layers. When impact energies exceed a certain critical value, the front aluminum layer surface is caved in in the vicinity of the impact point. The back surface aluminum layer is bulged out. In conjunction with this, one has the appearance of cracks perpendicular to the direction of fibers. From Fig.2, it is possible to see that the states of impact damage for the three types of samples are not greatly different. The surface area of damage and the size of the impact head are of the same order of magnitude. This is clearly different from resin based composite materials. Therefore, giving fibers an application of prestressing during solidification is certainly not capable of improving ARALL laminate counter impact properties.

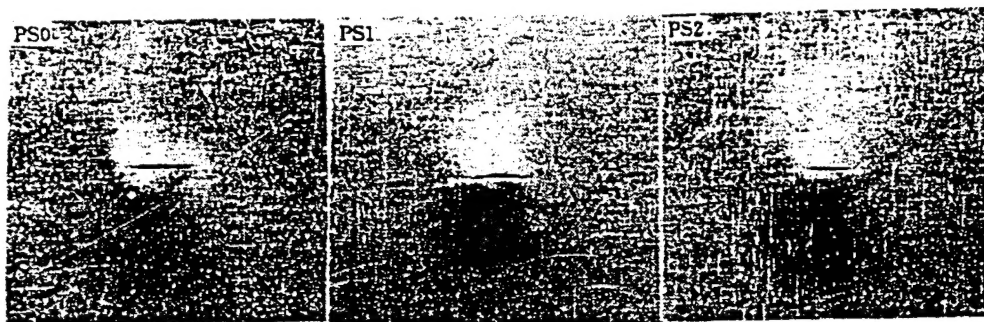


Fig.1 External View of ARALL Laminate Impact Damage (Back Surface)

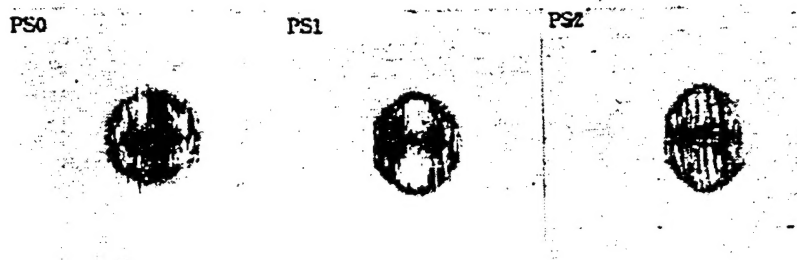


Fig.2 ARALL Laminate Impact Damage X Ray Penetration Photographs

2.2 Propagation of Impact Damage During Follow Up Fatigue Processes /1534

The propagation of ARALL laminate impact damage during follow on fatigue processes primarily appears as the opening of cracks on aluminum layer surfaces. Two types of delamination form between surface aluminum layers and adjacent aromatic fiber layers. The cracking of aluminum layer surfaces is given rise to by residual impact plastic deformation, and is not caused by the propagation of cracks caused by impact. The cracking associated with free ARALL laminate surface aluminum layers is a main crack passing through the impact point. During fatigue processes, there is rapid propagation in the direction of the width, and, in conjunction with that, penetration in the direction of the sample width. Prestressing of ARALL laminate surface aluminum layers is a dispersing of large numbers of mixed up small cracks in the vicinity of the impact point periphery. Propagation is slow. The opening of cracks in aluminum layer surfaces causes very, very great increases in shear stresses between layers in the vicinity of the cracking, setting off propagation of delamination between aluminum layers and aromatic fiber layers. Therefore the opening of cracks in aluminum layers is a primary cause producing delamination. However, inadequacies associated with the shear properties of adhesives between aluminum layers and aromatic fiber layers is the internal cause of delamination propagation. As a result, improving the shear properties of adhesives is capable of improving ARALL laminate fatigue properties after impact. During the entire fatigue process, no breakage of aromatic fibers was observed. In fatigue processes, impact

damage demonstrated that the opening of cracks on aluminum layer surfaces certainly did lead to the spreading of delamination between aluminum layer surfaces and adjacent aromatic fiber layers.

2.3 Fatigue Properties of ARALL Laminates after Impact

Fig.3 is the relationship curves associated with changes in dynamic stiffness over numbers of cycle iterations during fatigue processes after impact on three types of samples. From the Fig. it is possible to see that the patterns of drops in dynamic stiffnesses associated with free ARALL laminates and prestressed ARALL laminates are different. However, two types of laminates with different prestressing are the same. In initial cycle periods, drops in free laminate dynamic stiffness are very rapid. However, prestressed laminates are relatively stable. After going through a certain number of cycles, free laminates tend toward stability. However, prestressed laminates rapidly drop, finally coming together at a characteristic point. This can be explained as aluminum surfaces of prestressed laminates--during solidification processes--achieving residual stresses, thereby improving their fatigue properties. Following that, the number of cycle iterations increases. Cracks open in aluminum layers. Propagation of delamination causes residual stresses to be released. The result is that dynamic stiffness rapidly drops. Finally, it comes together with free laminates. At this time, the effects of prestressing have already completely disappeared.

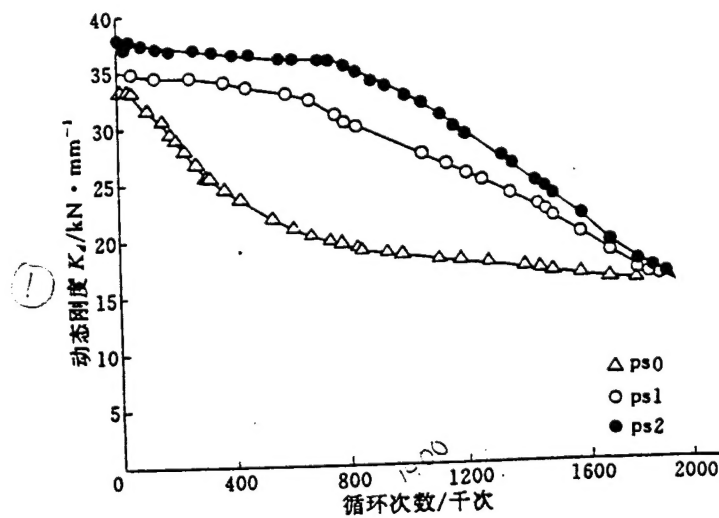


Fig.3 Dynamic Stiffnesses During Fatigue Processes After ARALL Laminate Impacts

Key: (1) Dynamic Stiffness (2) Number of Cycles/Thousand Iterations

The level of accumulated laminate damage during fatigue processes can be related to dynamic stiffnesses. It is possible to use the equation below to define degree of accumulated laminate damage.

$$D = 1 - (K_d / K_0) \quad (2)$$

In this, K_0 is initial dynamic laminate stiffness when fatigue begins. K_d is dynamic stiffness during fatigue processes. When fatigue begins, $D=0$. Through monitoring dynamic stiffness, it is possible to calculate accumulated levels of laminate damage during fatigue processes. Calculation results for three types of samples are the data points seen in Fig.4. From Fig.4, it can be seen that prestressed laminates and free laminates possess /1535 different patterns of accumulated damage. However, two types of samples with different prestressing have the same patterns of accumulated damage. Free laminate levels of accumulated damage (ps0) show power function changes with numbers of cycle iterations, that is,

$$D = 1 - \alpha \bar{N}^p \quad (3)$$

In this, \bar{N} is normalized numbers of cycle iterations. $\bar{N} = N_i / N_c$, N_c

is characteristic numbers of cycle iterations, that is, the confluence points of dynamic stiffness curves for free laminates and prestressed laminates. In this article, $N_c = 1.8 \times 10^6$. α and p are parameters awaiting specification.

Levels of accumulated damage for prestressed laminates (ps1 and ps2) show exponential change patterns, that is,

$$D = \zeta \eta^{\bar{N}} \quad (4)$$

In this, ζ and η are constants awaiting specification. The meanings of other symbols are as before. Using equations (3) and (4) on experimental results to carry out regression analysis, it is possible to obtain the cumulative damage functions for free laminates and prestressed laminates which follow

Free ARALL laminates

$$D = 1 - 0.475 \bar{N}^{0.2636} \quad (5)$$

Prestressed ARALL laminates

$$D = 0.02 \times (31.84 \bar{N}) \quad (6)$$

Cumulative damage functions are as shown by the solid lines in Fig.4. The experimental data points for two different types of prestressed samples fall on the periphery of the same curve drawn out, clearly showing that, after laminate prestressing reaches a certain level, continued addition of prestressing is certainly not capable of achieving better fatigue properties after impact.

3 Conclusions

ARALL laminate impact damage primarily appears as aromatic fiber breakage in the vicinity of impact points. Aluminum layers show the appearance of clear plastic deformations. In conjunction with this, there is a small area of delamination (of the same order of magnitude as the size of the impact head). Prestressing has no obvious improving effects on ARALL laminate counter impact damage capabilities.

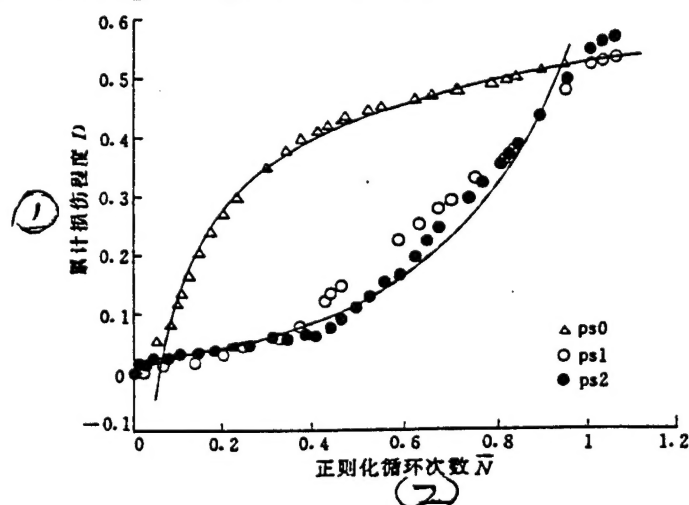


Fig.4 Cumulative Fatigue Damage Model for ARALL Laminates After Impact

Key: (1) Level of Cumulative Damage (2) Normalized Cycle Iteration Numbers

REFERENCE

- 1 柴兴国, 郭亚军. 复合材料层板冲击后压缩试验. 材料工程, 1991; (14): 29-31

(本卷终)

DISTRIBUTION LIST

DISTRIBUTION DIRECT TO RECIPIENT

<u>ORGANIZATION</u>	<u>MICROFICHE</u>
B085 DIA/RTS-2FI	1
C509 BALL0C509 BALLISTIC RES LAB	1
C510 R&T LABS/AVEADCOM	1
C513 ARRADCOM	1
C535 AVRADCOM/TSARCOM	1
C539 TRASANA	1
Q592 FSTC	4
Q619 MSIC REDSTONE	1
Q008 NTIC	1
Q043 AFMIC-IS	1
E404 AEDC/DOF	1
E410 AFDIC/IN	1
E429 SD/IND	1
P005 DOE/ISA/DDI	1
1051 AFIT/LDE	1
PO90 NSA/CDB	1

Microfiche Nbr: FTD95C000714
NAIC-ID(RS)T-0377-95